Alfvén vortices in Saturn's magnetosheath: Cassini observations

O. Alexandrova[1] and J. Saur[1]

Received 28 April 2008; revised 20 June 2008; accepted 25 June 2008; published 7 August 2008.

[1] First signatures of Alfvén vortices in the Kronian magnetosheath are presented. An Alfvén vortex is a non-linear bi-dimensional magnetic structure associated with sheared magnetic field and velocity perturbations, propagating obliquely to the external magnetic field direction. Such structures have been recently discovered by Cluster in Earth's magnetosheath downstream of a quasi-perpendicular bow-shock at scales close to $10c/\omega_{pi}$ (where c is the speed of light and ω_{pi} the ion plasma frequency). The presence of Alfvén vortices downstream of a quasi-perpendicular bow-shock of Saturn with comparable scales to the ones at Earth indicates the universality of this phenomenon. It suggests that such non-linear structures are an inherent property of plasma flow downstream of collisionless shock waves, which can have broad astrophysical applications. **Citation:** Alexandrova, O., and J. Saur (2008), Alfvén vortices in Saturn's magnetosheath: Cassini observations, *Geophys. Res. Lett.*, *35*, L15102, doi:10.1029/2008GL034411.

1. Introduction

[2] A planetary magnetosheath contains shocked and decelerated solar wind plasma with a high level of magnetic fluctuations. The intensity and the origin of these fluctuations depend on the upstream bow-shock geometry. When the solar wind magnetic field $\mathbf{B_{sw}}$ is quasi-parallel to the local shock normal $\mathbf{n}$, fluctuations coming from the solar wind penetrate downstream after being amplified and modified within the quasi-parallel shock front. If the angle between $\mathbf{n}$ and $\mathbf{B_{sw}}$ is large, $\Theta_{BN} \in (45, 90)°$, (quasi-perpendicular configuration), the downstream fluctuations are generated mainly locally. It is widely accepted that, in the last situation, the main source of the fluctuations is the ion temperature anisotropy, which generates low frequency (with respect to the ion cyclotron frequency f_{ci}) Alfvén-Ion-Cyclotron (AIC) and mirror quasi-linear waves [*Schwartz et al.*, 1996]. Therefore, the usual interpretation of the magnetosheath fluctuations downstream of a quasi-perpendicular shock is a superposition of weakly interacting linear waves, i.e., in terms of weak turbulence [*Rezeau et al.*, 1999].

[3] Recently, Cluster observations revealed the existence of strongly non-linear coherent structures in the form of Alfvén vortices in the terrestrial magnetosheath [*Alexandrova et al.*, 2006]. An Alfvén vortex is a bi-dimensional magnetic structure (with wave vectors $k_\perp \gg k_\parallel$) associated with sheared magnetic field and plasma velocity perturbations $\delta B_\perp$, $\delta V_\perp$ (where $\perp$ and $\parallel$ denote perpendicular and parallel directions to a mean field, respectively). It propagates obliquely to the external magnetic field $\mathbf{B_0}$, in contrast to AIC waves, which are expected to have $k_\parallel \gg k_\perp$. The simplest interpretation of such structures is given within the incompressible non-linear MHD equations [*Petviashvili and Pokhotelov*, 1992].

[4] In the Earth's magnetosheath, the Alfvén vortices are observed at spatial scales of the order of $10c/\omega_{pi}$ and are associated with a local decrease of the amplitudes of the longitudinal fluctuations $\delta B_\parallel$, indicating a low level of plasma compression within the vortices. Their amplitude is observed to be small but finite, $\delta B_\perp/B_0 \sim 0.1$ and the propagation velocity in the plane nearly perpendicular to $\mathbf{B_0}$ is estimated to vary in the range $[0, 0.3]V_A$, V_A being the Alfvén speed [*Alexandrova et al.*, 2006].

[5] In the solar wind, the signatures of Alfvén vortices at scales close to the ion characteristic scales have not been observed, up to now, suggesting that the presence of the bow shock plays a crucial role in their appearance. To check this idea we study here magnetic fluctuations measured by the Cassini spacecraft, downstream of Saturn's bow-shock. Since Cassini is not a multi-spacecraft mission, such as Cluster, and due to the absence of plasma data, our identification of Alfvén vortices at Saturn relies on the similarities of the observed spectral features and magnetic waveforms at Earth and Saturn.

[6] The properties of the bow-shock and solar wind at Saturn are very different compared to those at Earth, the shock being stronger (the Mach number is higher) and the solar wind magnetic field and density smaller by two orders of magnitude. If, despite these important differences, the Alfvén vortices are still present downstream of the bow-shock of Saturn that may mean that such non-linear structures are an inherent property of plasma flows downstream of collisionless shock waves.

2. Selected Time Period

[7] We analyze magnetic field fluctuations within the Kronian magnetosheath using high resolution magnetic field data measured by Cassini/MAG instrument [*Dougherty et al.*, 2004]. Wavelet decomposition is an effective tool for the analysis of fluctuating (or turbulent) fields. The wavelet coefficients of the i-th component of the magnetic field are $\mathcal{W}_i(\tau, t) = \sum_{j=0}^{N-1} B_i(t_j)\psi[(t_j - t)/\tau]$, where t is a time variable and τ is a time scale (i.e., inversed frequency $1/f$). In our study we use $\psi(u) = \pi^{-1/4} \exp(-i\omega_0 u) \exp(-u^2/2)$, the Morlet mother wavelet. This function has a form similar to the Alfvén vortices, and so it allows the most efficient identification of such structures in a turbulent signal. The quantity $\mathcal{W}_i^2(\tau, t)$ gives the energy of the fluctuations at a given time and scale. We approximate the energy of the longitudinal fluctuations $\mathcal{W}_\parallel^2(\tau, t)$ to be equal to the square of the wavelet coefficients of the magnetic field modulus

[1]Institute of Geophysics and Meteorology, University of Cologne, Cologne, Germany.

0094-8276/08/2008GL034411

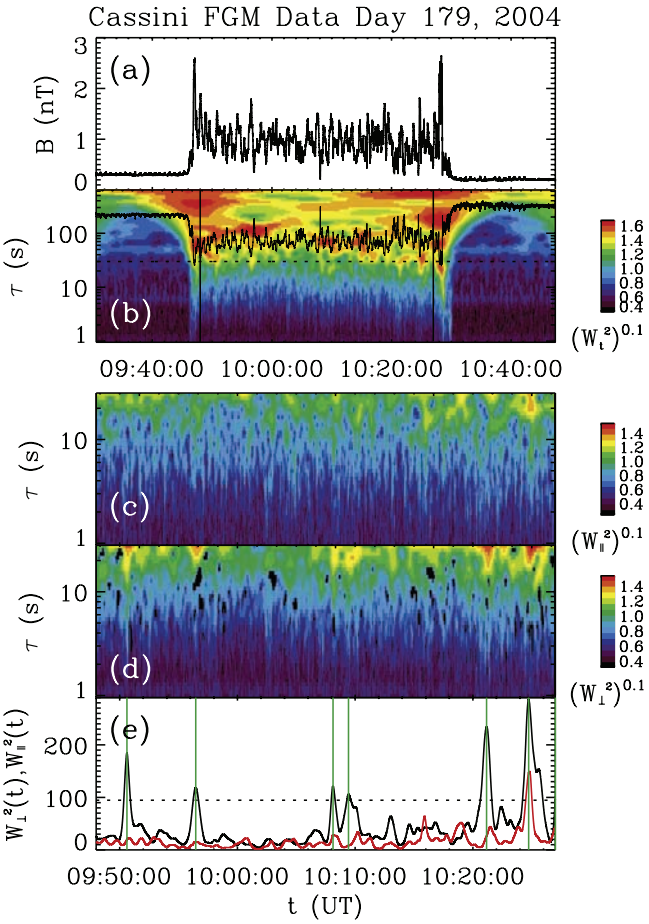

Figure 1. (a) Magnetic field strength for the time interval [09:30–10:48] UT on June 27, 2004. (b) Morlet wavelet scalogram of the total energy of magnetic fluctuations; the vertical lines bracket the magnetosheath time interval [09:48–10:27] UT analyzed in the paper while the horizontal dotted line corresponds to a time scale of 30 s, the solid line is the proton gyration period. (c) Scalogram of the energy of the longitudinal fluctuations $W_{\|}^2(\tau, t)$ for the magnetosheath interval and for the scales $1 \leq \tau \leq 30$ s. (d) Scalogram of $W_{\perp}^2(\tau, t)$ for the same interval and scales as Figure 1c. (e) Result of integration of the upper scalograms over scales, $W_{\perp}^2(t)$ (black line) and $W_{\|}^2(t)$ (red line) (we avoid the scale $\tau = 1$ s, where the turbulence level is of the order of the FGM sensitivity 10^{-4} nT^2/Hz); vertical lines indicate the central time t_0 of the energetic events with $W_{\perp}^2(t) > 2\langle W_{\perp}^2(t)\rangle$, the threshold shown by a horizontal dotted line.

$\mathcal{W}_{|B|}^2(\tau, t)$. This is a good approximation for $\delta B^2 \ll B_0^2$. The energy of the transverse fluctuations is $\mathcal{W}_{\perp}^2 = \mathcal{W}_{tot}^2 - \mathcal{W}_{\|}^2$, where $\mathcal{W}_{tot}^2 = \sum_{i\,=\,x,y,z} \mathcal{W}_i^2(\tau, t)$ is the total energy of the fluctuations.

[8] Comparing the magnitude of $\mathcal{W}_{\perp}^2$ with respect to $\mathcal{W}_{\|}^2$ within the magnetosheath crossings during the first two Cassini orbits, we arrive at the following picture: In the inner magnetosheath, the turbulence is dominated by large amplitude longitudinal fluctuations, probably associated with the mirror mode structures previously observed in Saturn's magnetosheath by Voyager-2 [*Bavassano Cattaneo et al.*, 1998]. However, just downstream of the bow-shock (in the outer magnetosheath), the Alfvénic fluctuations dominate a broad range of scales forming an *Alfvénic region*. In the following, we present a detailed analysis of magnetic fluctuations within one of these Alfvénic regions.

[9] To be sure that the Cassini spacecraft is in the outer magnetosheath, we select a time interval in-between of two shock crossings with a relative short duration of about one hour. Figure 1 shows an example of such an interval, which contains the 1st and the 2nd shock crossings during Saturn Orbit Insertion. The first bow-shock crossing (S1) occurs at 09:46:46 UT at a radial distance of 49.14 R_S from the planet, the second crossing (S2) occurs at 10:28:34 UT, at a radial distance of 48.84 R_S. Both shocks are crossed at local time of 07:33. These shocks have been identified by *Dougherty et al.* [2005]. *Achilleos et al.* [2006] analysed these crossings in details and determined $\Theta_{BN} \simeq 60°$ for both shocks, i.e., a quasi-perpendicular geometry. The upstream plasma β is 0.25 for S1 and 0.44 for S2, the upstream ion inertial length is estimated to be $c/\omega_{pi} \sim 1200$ km for both shocks. The solar wind magnetic field is 0.3 nT, and downstream of S1 it increases up to $B_0 = 1.2$ nT. Assuming the solar wind velocity to be 400 km/s, the magnetosonic Mach numbers are 10 and 14 for S1 and S2, respectively.

3. Signatures of Alfvén Vortices

[10] For the selected time interval, Figure 1b shows the distribution of the total energy of magnetic fluctuations in the time–scale plane. The scales range from 1 to 600 seconds and the amplitude levels are represented by a color scale. The proton cyclotron period, T_{cp}, is presented by a black solid line. Just below T_{cp}, in the vicinity of the horizontal dotted line at $\tau = 30$ s, one observes a set of localized energetic events, which, by analogy with the terrestrial case [see *Alexandrova et al.*, 2006] can be Alfvén vortices.

[11] Let us see if these intermittent events are indeed Alfvénic, with $\delta B_{\perp}^2 \gg \delta B_{\|}^2$. In our case, the separation in parallel and transverse energies with respect to a mean field, as explained in section 2, is possible at scales smaller than 30–35 s, where the amplitudes of the fluctuations verify $\delta B < B_0$. For the time interval indicated by the two vertical solid lines in Figure 1b and scales below the horizontal dashed line ($\tau \leq 30$ sec), Figures 1c and 1d display the scalograms of $\mathcal{W}_{\|}^2(\tau, t)$ and $\mathcal{W}_{\perp}^2(\tau, t)$, respectively. Figure 1e shows the integral of $W_{\perp}^2(\tau, t)$ (black line) and of $W_{\|}^2(\tau, t)$ (red line) over the time scales $2 \leq \tau \leq 30$ s. Vertical (green) lines indicate the central time t_0 of the energetic events with $W_{\perp}^2(t) > 2\,\langle W_{\perp}^2(t)\rangle$, where $\langle . \rangle$ denotes the averaging over the time variable. We can see that most of the events are Alfvénic, i.e., $W_{\perp}^2(t) \gg W_{\|}^2(t)$ (except the last one). Their properties are collected in Table 1.

[12] To complete the statistical picture of the magnetosheath fluctuations, we compute a power spectral density (PSD) of the whole magnetosheath crossing (Figure 2a) and around each selected energetic event. Figure 2b gives an example for event 4. In both plots, the total PDS, S, is shown by solid lines; the dashed and dash-dotted lines display the PSD of the perpendicular and the longitudinal fluctuations, $S_{\perp}$ and $S_{\|}$, respectively. The mean magnetosheath spectrum follows a f^{-3}–power law at frequencies

Table 1. Properties of the Alfvénic Energetic Events[a]

Event	t_0 (UT)	τ_0 (s)	λ_i/λ_{max}	Θ (degree)
1	09:50:36	34	(1, 0.1, 0.05)	25
2	09:56:27	30	(1, 0.2, 0.04)	85
3	10:08:07	20	(1, 0.6, 0.06)	60
4	10:09:26	20	(1, 0.8, 0.09)	40
5	10:21:09	30	(1, 0.7, 0.17)	25
6	10:24:44	32	(1, 0.4, 0.04)	50

[a]Here t_0 is the central times of the events, τ_0 is their time scale, λ_i/λ_{max} are the normalized variance eigenvalues of $\delta\mathbf{B}$ calculated for a $2\tau_0$ time interval around each t_0, Θ is an angles between $\mathbf{e}_{min}$ and the local $\mathbf{B}_0$ within each analyzed interval.

above 0.06 Hz. Below this frequency broad spectral features appear, while the local spectrum of Figure 2b shows a clear spectral knee around $f_0 = 0.04$ Hz. In the terrestrial magnetosheath, such spectral knees appear in the presence of Alfvén vortices and the central frequency of the knee corresponds to the vortex radius. Here, the central frequency of the spectral knee varies from event to event, explaining the absence of a clear knee in the spectrum of the whole magnetosheath crossing.

[13] The bottom plots of Figure 2 show the ratio $S_\parallel/S$ for the corresponding upper plots. This quantity represents the level of compressibility of the fluctuations at different frequencies. For the whole magnetosheath crossing $S_\parallel/S$ reaches its minimum of 0.2 between 0.03 and 0.04 Hz. For the local spectrum we observe a decrease of $S_\parallel/S$ down to zero in the vicinity of the spectral knee. Similar behaviors is observed for the terrestrial Alfvén vortices, revealing their incompressible nature, even within the compressible magnetosheath plasma [*Alexandrova*, 2008].

[14] Let us now analyze the magnetic waveforms at scales corresponding to the spectral knee. Since the central frequency (or the wavelet scale $\tau_0 = 1/f_0$) varies from event to event (see Table 1) and because of the limited sensitivity of the MAG instrument, we define the magnetic fluctuations of the spectral knee as

$$\delta B_i(t) = \langle B_i(t) - \langle B_i(t)\rangle_{\tau_0}\rangle_{\tau_1} \quad (1)$$

with $\tau_1 < \tau_0$. Here, the smoothing operation over time periods τ_0 and τ_1 is defined as $\langle X(t)\rangle\tau = \frac{1}{N}\sum_{j=0}^{N-1} X(t_j - t)$, N being the number of data points within the period τ_0 and τ_1, respectively. This definition is used to avoid the fluctuations on scales larger ($\tau > \tau_0$) than those of the events we are analyzing; τ_1 is chosen to be 2 s in order to avoid aliasing presented at high frequencies.

[15] Figure 3a shows the properties of $\delta\mathbf{B}$ during the 1st and 3rd energetic events (taken as representative examples): The top plots show three components of the fluctuations in the minimum variance frame [*Sonnerup and Scheible*, 1998] and the bottom plots show the hodograms in the plane perpendicular to the minimum variance direction $\mathbf{e}_{min}$. The magnetic fluctuations have coherent waveforms, similar to that observed in the Earth's magnetosheath during Alfvén vortex crossings. In contrast to events at Earth, here the fluctuations have large amplitudes, $\delta B/B_0 \sim 0.5$, and we observe small-scale perturbations superposed on the principal structures.

[16] The Alfvén vortices identified in the terrestrial magnetosheath show a quasi-circular polarization in the vortex plane, which can be determined as the plane orthogonal to the minimum variance direction. For most of the events studied here, in the plane perpendicular to $\mathbf{e}_{min}$, we observe the polarization, similar to the terrestrial structures (see the hodogram for event 3 in Figure 3a). However, for the first two events we observe a quasi linear polarization (see the hodogram for event 1). Such polarization can be observed when the spacecraft passes through an Alfvén vortex close to its center, where $\mathbf{e}_{min}$ is not always well

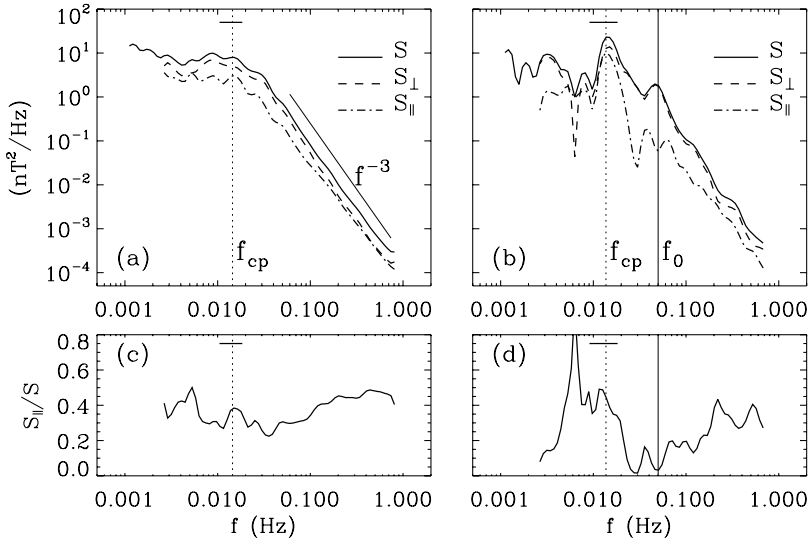

Figure 2. (a) The total power spectral density (PSD) of magnetic fluctuations S (solid line) for the studied magnetosheath interval, $S_\perp = \mathrm{PSD}(\delta B_\perp)$ (dashed line) and $S_\parallel = \mathrm{PSD}(\delta B_\parallel)$ (dash-dotted line), vertical dotted line indicates a mean value of the proton cyclotron frequency, $f_{cp} \simeq 0.015$ Hz, its standard deviation is shown by a solid horizontal line. (b) The same as Figure 2a but for an interval of 1 min around $t_0 = 10{:}09{:}26$ UT, f_0 is a central frequency of the spectral knee. (c and d) The ratio $S_\parallel(f)/S(f)$ for Figures 2a and 2b, respectively.

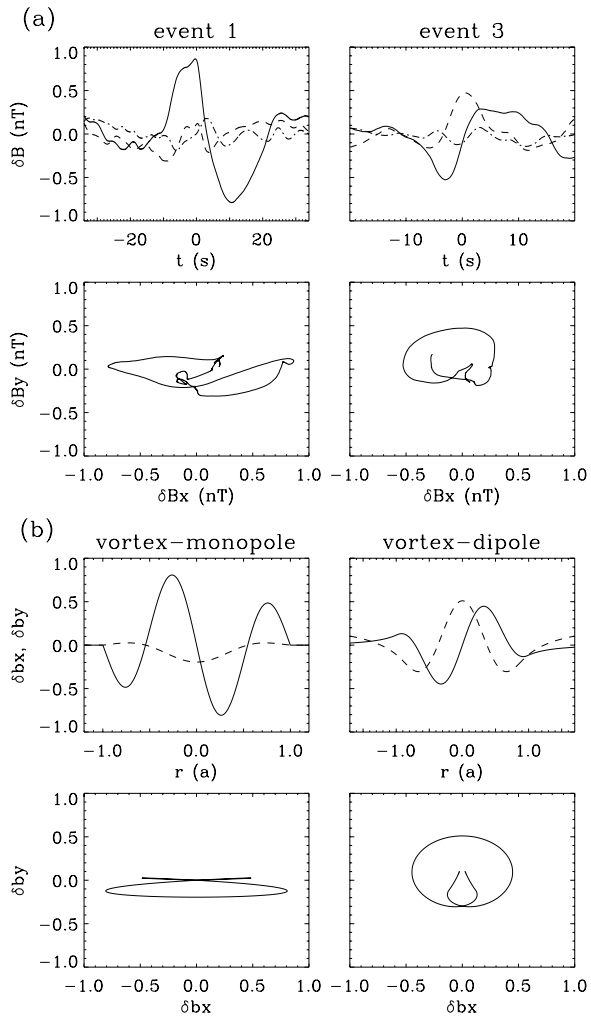

Figure 3. (a) Magnetic fluctuations in the minimum variance frame and polarization in the plane orthogonal to $\mathbf{e}_{\min}$ for events 1 and 3; $\delta\mathbf{B}$ is calculated with equation (1) on time intervals $2\tau_0$ (i.e., 68 s for event 1 and 40 s for event 3); δB_x (solid), δB_y (dashed) and δB_z (dash-dotted) are the components along the directions of maximum, intermediate and minimum variance, respectively. (b) Simulated magnetic field and polarization properties of monopole and dipole vortices passed by a probe along y-axis; δb_x (solid line) and δb_y (dashed line).

defined: In such a case, $\mathbf{e}_{\min}$ may indicate the direction of the satellite path in the vortex plane and not the normal to the plane.

[17] There are two independent Alfvén vortex topologies: monopole and dipole [*Petviashvili and Pokhotelov*, 1992]. The monopole vortex is characterized by a parallel (to the ambient field) vector potential $A \sim (J_0(kr) - J_0(ka))$, for the radial distance $r < a$, and $A = 0$ for $r > a$, with a being the radius of the vortex, k is given by the condition $J_1(ka) = 0$, and J_0 and J_1 are the Bessel functions of 0th and 1st order. The dipole vortex is described by $A \sim J_1(kr)/J_0(ka)$ for $r < a$, and $A \sim 1/r$ for $r > a$.

[18] To further support the identification of Alfvén vortices, we compare the observed fluctuations with theoretically expected fields. Left plots of Figure 3b show the magnetic field of a monopole Alfvén vortex passed by a probe along the y coordinate with the closest approach to the center $\Delta x \simeq 0.04\ a$. Here, the magnetic field component δb_x matches well the observed profile of the principal magnetic fluctuations of event 1. The polarization details are difficult to compare as far as in our observations there are small scale perturbations superimposed on the principal structure. Right plots of Figure 3b show the field of a dipole Alfvén vortex crossed along y and with $\Delta x \simeq 0.2\ a$. Here, both components of the vortex field and polarization properties match well the field and polarization of event 3.

[19] The vortex transverse dimension, a, cannot be determined exactly with a single spacecraft, but can be estimated from information about the terrestrial structures. Alfvén vortices in the Earth's magnetosheath are mostly convected by the plasma flow V passed the spacecraft [*Alexandrova et al.*, 2006], and so the spatial characteristic scale of a vortex is $a \simeq V\tau_0$. Unfortunately, we have no simultaneous measurements of the ion moments by Cassini available. However, from observations by Voyager-2 we know that downstream of Saturn's quasi-perpendicular bow-shock, the plasma bulk velocity is close to 125 km/s and the ion plasma density is of the order of 0.5 cm^{-3} [*Bavassano Cattaneo et al.*, 1998], which corresponds to an ion inertia length $c/\omega_{pi} \simeq 320$ km. Thus a rough estimate of the transverse scale of the events analyzed in this letter gives $a \in [2.5, 4.0] \times 10^3$ km, or $a \in [8,12]\ c/\omega_{pi}$. This is of the same order of magnitude as the transverse scale of the Alfvén vortices observed by Cluster in the Earth's magnetosheath.

4. Conclusion and Discussion

[20] In this letter we present the first observations of signatures of Alfvén vortices in the Kronian magnetosheath downstream of a quasi-perpendicular bow-shock. Since an Alfvén vortex contains a localized current, a spacecraft measures coherent, time localized, magnetic fluctuations while flying through such a structure. In a magnetic spectrum, these structures appear as a local maximum at frequencies corresponding to their Doppler shifted characteristic spatial scale.

[21] The presence of Alfvén vortices in the magnetosheath of Saturn, at the same spatial scale as the vortices in the terrestrial magneosheath, $\sim 10c/\omega_{pi}$, indicates that these structures are an inherent property of plasma flow downstream of collisionless shock waves, at least for its quasi-perpendicular portion.

[22] The absence of Alfvén vortex signatures in the inner magnetosheath (at least for the first two Cassini orbits around Saturn's magnetosphere) may be due to particular plasma conditions at ~9.5 AU, i.e., in a medium with a low mean field, the Alfvén vortices with large amplitudes ($\delta B/B_0 \sim 0.5$) are not stable, i.e., their life time is smaller than the convection time in the magnetosheath.

[23] The last point that we like to stress concerns the shape of the magnetic spectrum above f_{ci}. In the case of the Earth, this spectrum is a well-defined power law with a mean spectrum close to f^{-3} [*Czaykowska et al.*, 2001]. At Saturn, the mean magnetosheath spectrum reported here follows the same law, indicating the universality of plasma flow behind the collisionless shock wave.

[24] **Acknowledgments.** We acknowledge usage of Cassini spacecraft magnetic field data (P.I. M. K. Dougherty) which we received from the Planetary Data System. The Wavelet software was provided by C. Torrence and G. Compo, and is available at http://paos.colorado.edu/research/wavelets/.

References

Achilleos, N., et al. (2006), Orientation, location, and velocity of Saturn's bow shock: Initial results from the Cassini spacecraft, *J. Geophys. Res.*, *111*, A03201, doi:10.1029/2005JA011297.

Alexandrova, O. (2008), Solar wind vs magnetosheath turbulence and Alfvén vortices, *Nonlinear Processes Geophys.*, *15*, 95–108.

Alexandrova, O., A. Mangeney, M. Maksimovic, N. Cornilleau-Wehrlin, J.-M. Bosqued, and M. André (2006), Alfvén vortex filaments observed in magnetosheath downstream of a quasi-perpendicular bow shock, *J. Geophys. Res.*, *111*, A12208, doi:10.1029/2006JA011934.

Bavassano Cattaneo, M. B., C. Basile, G. Moreno, and J. D. Richardson (1998), Evolution of mirror structures in the magnetosheath of Saturn from the bow shock to the magnetopause, *J. Geophys. Res.*, *103*, 11,961–11,972, doi:10.1029/97JA03683.

Czaykowska, A., T. M. Bauer, R. A. Treumann, and W. Baumjohann (2001), Magnetic field fluctuations across the Earth's bow shock, *Ann. Geophys.*, *19*, 275–287.

Dougherty, M. K., et al. (2004), The Cassini magnetic field investigation, *Space Sci. Rev.*, *114*, 331–383, doi:10.1007/s11214-004-1432-2.

Dougherty, M. K., et al. (2005), Cassini magnetometer observations during Saturn orbit insertion, *Science*, *307*, 1266–1270, doi:10.1126/science.1106098.

Petviashvili, V. I., and O. A. Pokhotelov (1992), *Solitary Waves in Plasmas and in the Atmosphere*, Gordon and Breach Sci., Philadelphia, Pa.

Rezeau, L., G. Belmont, N. Cornilleau-Wehrlin, F. Reberac, and C. Briand (1999), Spectral law and polarization properties of the low-frequency waves at the magnetopause, *Geophys. Res. Lett.*, *26*, 651–654, doi:10.1029/1999GL900060.

Schwartz, S. J., D. Burgess, and J. J. Moses (1996), Low-frequency waves in the Earth's magnetosheath: Present status, *Ann. Geophys.*, *14*, 1134–1150.

Sonnerup, B., and M. Scheible (1998), Minimum and maximum variance analysis, in *Analysis Methods for Multi-Spacecraft Data*, edited by G. Paschmann and P. W. Daly, pp. 185–220, Int. Space Sci. Inst., Bern, Switzerland.

O. Alexandrova and J. Saur, Institute of Geophysics and Meteorology, University of Cologne, D-50923 Cologne, Germany. (alex@geo.uni-koeln.de; saur@geo.uni-koeln.de)